NAVAL MEDICAL RESEARCH UNIT SAN ANTONIO

JOINT REPORT

RAPID IDENTIFICATION OF BACTERIAL PATHOGENS OF MILITARY INTEREST USING SURFACE-ENHANCED RAMAN SPECTROSCOPY

Rene Alvarez[1], PhD; Alexander J. Burdette[1], PhD; Xiaomeng Wu[2], BS; Christian Kotanen[1], PhD; Yiping Zhao[2], PhD; Ralph A. Tripp[3], PhD

[1] Immunodiagnostics and Bioassay Development Department, Combat Casualty Care and Operational Medicine Directorate, Naval Medical Research Unit San Antonio, Ft. Sam Houston, TX

[2] Department of Physics and Astronomy, University of Georgia, Athens, GA

[3] Department of Infectious Diseases, College of Veterinary Medicine, University of Georgia, Athens, GA

NAMRU-SA REPORT #2014-58

Reviewed and Approved by:

6/13/2014
Date

Rene Alvarez, Ph.D.
Director, Combat Casualty Care & Operational Medicine
Chair, Scientific Review Board
Naval Medical Research Unit San Antonio
3650 Chambers Pass, BLDG 3610
Fort Sam Houston, TX 78234-6315

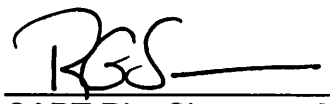

19 JUN 14
Date

CAPT Rita Simmons, MSC, USN
Commanding Officer
Naval Medical Research Unit San Antonio
3650 Chambers Pass, BLDG 3610
Fort Sam Houston, TX 78234-6315

Table of Contents

Executive Summary

Background: The presence of bacterial infections in combat-related injuries in warfighters is becoming increasingly more common and severe. Thus, quick and accurate detection of the invading pathogen is needed so appropriate treatment plans can be generated to improve the prognosis of wounded warriors.

Objective: The purpose of this study was to evaluate the feasibility of utilizing Surface-Enhanced Raman Spectroscopy (SERS) for the detection and generation of "molecular fingerprints" of military relevant microorganisms often associated with wound infections.

Methods: A total of sixteen bacterial isolates including: six *Acinetobacter baumannii,* four *Staphylococcus aureus,* three *Klebsiella pneumonia,* and three *Pseudomonas aeruginosa* strains were evaluated for the generation of SERS-based "molecular fingerprints" followed by Principal Component Analysis to determine the uniqueness and commonalities of each spectra. Quantitative polymerase chain reaction (qPCR) with melting curves was used to validate the SERS spectra.

Results: Our data demonstrate that SERS could not only generate unique "molecular fingerprints" for these organisms in 15-30 seconds, but could also appropriately group organisms based on commonalities. These data were confirmed by quantitative real-time PCR amplification utilizing species specific primers.

Conclusions: Study results demonstrate the valuable potential for a SERS-based platform to rapidly detect microorganisms of military significance. The data demonstrate that SERS can be used to accurately discriminate between bacterial species in a quick and efficient manner. This report sets the foundation for the utilization of a SERS platform for rapid detection of microorganisms of military relevance, which may ultimately lead to the development of a field deployable point-of-care handheld detection system.

Introduction

As of March 2011, the wars in Iraq and Afghanistan have resulted in substantial morbidity and mortality including a total of 4,444 deaths and 32,044 wounded in action during Operation Iraqi Freedom and Operation New Dawn, and 1,505 deaths and 10,749 wounded in action during Operation Enduring Freedom in Afghanistan (Aronson, Sanders, & Moran, 2006). Because of the nature of combat injuries caused by improvised explosive devices, mortars, rocket-propelled grenades, and gunshots while wearing protective gear, extremity wounds were prevalent with infections continuing to be a major cause of excess morbidity and mortality (Aronson et al., 2006). According to the Joint Theater Trauma Registry, approximately 25% of combat casualties were found to develop an infection, with the rate approaching 50% in wounded warriors requiring intensive care treatment (Aronson et al., 2006).

Infections are commonly associated with methicillin-resistant *Staphylococcus aureus* (MRSA) and gram-negative bacteria, specifically the multidrug resistant *Acinetobacter baumannii-calcoaceticus* complex, which remains a critical cause of infection. Additionally, there has been a dramatic increase of infections associated with extended-spectrum β-lactamase-producing bacteria, including *Escherichia coli*, *Klebsiella pneumoniae*, and multidrug resistant *Pseudomonas aeruginosa* (Aronson et al., 2006). The breadth of infection of these wounds has been a significant factor in determining antibiotic prophylaxis and treatment. Current diagnostic assays used to dictate disease intervention strategies are limited in sensitivity, have a poor predictive value, or are time consuming. Thus, there is a critical, yet unmet need for a rapid and sensitive means of diagnosing bacterial agents that inflict a significant burden on our warfighters.

Conventional protocols for diagnosing bacterial infections require (1) isolation of a pure culture of the bacterium, (2) subsequent determination of the identity of the isolate, and (3) examination of the isolate's responses to various antibiotics or selection media. Such a process often requires days to weeks, or even months for some slow growing bacteria. Over the past decade, several polymerase chain reaction (PCR)-based methods have been developed for both the identification of bacteria (Mothershed

& Whitney, 2006) and the genes that confer antibiotic resistance (Rolain, Mallet, Fournier, & Raoult, 2004).

Although such genotypic approaches are compelling, the assays typically require species and/or strain specific probes that may or may not be available for a particular organism. Mass spectrometry is also a culture-free approach and can give proteomic information of the bacteria. Like PCR, mass spectrometry depends on the available prior knowledge on the pathogens, which may or may not exist. Surface-Enhanced Raman Spectroscopy (SERS) has emerged as a powerful analytical tool that extends the possibilities of surface vibrational spectroscopy to solve a vast array of chemical problems. Since its discovery in the 1970's (Albrecht & Creighton, 1977; Fleischmann, Hendra, & McQuillan, 1974; Jeanmaire & Van Duyne, 1977), SERS has matured into a widely used technique, especially in biosensing and medical diagnostics. It has been widely used in the analysis of drug mixtures and active ingredients, identification of contaminants, and exploration of drug-excipient interactions (Pinzaru, Pavel, Leopold, & Kiefer, 2004).

Additionally, SERS has been used to identify different vitamins (Failloux, Bonnet, Baron, & Perrier, 2003; Wang, Li, Zhang, & An, 2003, 2004), alkaloids (Pavel, Szeghalmi, Moigno, Cinta, & Kiefer, 2003; Sagmuller, Schwarze, Brehm, Trachta, & Schneider, 2003), antimicrobial agents (Iliescu, Cinta, & Kiefer, 2000; Lecomte & Baron, 1997; Lecomte, Moreau, Manfait, Aubard, & Baron, 1995), anti-tumor agents (Streltsov et al., 2003; Vivoni, Chen, Ejeh, & Hosten, 2001), etc. under different environments such as pH dependence, solvent dependence, surface interaction, and such. SERS has also been used for DNA and RNA detection in biological systems (Allain & Vo-Dinh, 2002; Faulds, Smith, & Graham, 2005; Macaskill et al., 2007; Pal, Isola, Alarie, Stokes, & Vo-Dinh, 2006; Vo-Dinh, Allain, & Stokes, 2002), specifically for the detection of viruses (Driskell et al., 2008; Shanmukh et al., 2006) and bacteria (Chu, Huang, & Zhao, 2008; Jarvis, Clarke, & Goodacre, 2006; Kahraman, Yazici, Sahin, Bayrak, & Culha, 2007; Pearman & Fountain, 2006). In this report, we evaluated the ability of SERS to differentiate between bacterial species of military importance using qPCR as validation.

Materials and Methods

Silver nanorod (AgNR) fabrication

SERS spectra were acquired using AgNR array substrates fabricated by the oblique angle deposition (OAD) technique using a custom-designed electron beam/sputtering evaporation (e-beam) system (Chaney, Shanmukh, Dluhy, & Zhao, 2005; Driskell et al., 2008; Liu, Chu, & Zhao, 2010). Briefly, glass microscopic slides (Gold Seal® Catalog No.3010, Becton, Dickinson and Company, Portsmouth, NH) used for AgNR arrays deposition were cleaned with piranha solution (80% sulfuric acid, 20% hydrogen peroxide in volume) and rinsed with deionized water. The substrates were then dried with a stream of nitrogen before being loaded into the e-beam deposition system. A 20-nm titanium film, followed by a 200-nm silver film layer were first evaporated onto the glass slides at a rate of ~0.2 nm/s and 0.3 nm/s, respectively, while the substrate surface was held perpendicular to the incident vapor direction. The substrates were then rotated to 86° with respect to the incident vapor and AgNRs were grown at this oblique angle with a deposition rate of ~0.3 nm/s. The film thickness was monitored in situ by a quartz crystal microbalance (QCM) positioned at normal incidence to the vapor source direction. The thickness of the AgNR layer was set to be 1000 nm for standard substrates.

Bacteria incubation and preparation

Sixteen diverse bacteria were received from Brooke Army Medical Center (Joint Base San Antonio, Ft. Sam Houston, TX) and used in this study (Table 1). Each bacterial isolate was stored in glycerol stocks (20 aliquots for each strain) at -80°C. The stocks were a 1:1 mixture of bacterial culture and 50% glycerol in PBS yielding a final glycerol content of 25%. Bacteria from glycerol stocks were transferred to trypticase soy broth (TSB, Difco, Detroit, MI) for growing overnight at 37°C. Overnight cultures were spread on plate count agar and incubated overnight at 37°C (PCA, Difco, Detroit, MI) for colony isolation. A single colony of bacteria was incubated in TSB overnight at 37°C to yield generally ~10^9 CFU/ml. Following incubation, the cultures were washed three times with sterile deionized (DI) water before re-suspending in sterile DI water. Next, 2 µl of the bacterial solution was pipetted onto the SERS substrate and dried in a biosafety level 2 safety cabinet.

SERS measurements and data analysis

SERS spectra were acquired using a portable Enwave Raman system (Model ProRaman 785A2, Enware Optronics Inc., Irvine, CA), with a 785 nm near-IR diode laser as the excitation source. The power of the laser at the sample was set to be ~ 60 mW. SERS spectra over a range of ~ 400 – 1800 cm^{-1} was used over a five second exposure time. SERS spectra were collected from nine spots (3 × 3 array) across the substrate surface and multiple substrates were measured. All data analysis was performed using Origin software 8.5 version (OriginLab Corporation, Northampton, MA). Principal component analysis (PCA) and Cluster analysis (Ward's method) were conducted with Matlab 2000b (The MathWorks, Inc., Natick, MA) using the PLS toolbox (Eigenvector Research, Inc., Wenatchee, WA).

Bacterial genomic DNA isolation and quantitative PCR (qPCR)

Bacterial strains were grown in tryptic soy broth overnight at 37°C. Cultures were pelleted by centrifugation at 4,000 x g for 15 minutes and genomic DNA was isolated using the Sigma GenElute™ Bacterial Genomic DNA kit (Sigma-Aldrich, St. Louis, MO) according to manufacturer's instructions. Lysozyme treatment was used for *Acinetobacter baumannii* prior to cell lysis, while lysostaphin and lysozyme were used for *Staphylococcus aureus*. Cells were then lysed, treated with Rnase A, and genomic DNA was purified through a spin-column format and quantified. For qPCR analysis, bacterial DNA was amplified in a 20 µl reaction using Sybr green PCR mastermix (Invitrogen, Carlsbad, CA) with 300 nM primers per reaction in technical duplicates. The sequences for the primers utilized are listed in table 2. PCR cycling parameters were performed on an Eppendorf Realplex4 Mastercycler® (Eppendorf, Hauppauge, NY) utilizing two-step PCR with an initial denaturation step at 95°C for 10 minutes, followed by 40 cycles of 95°C for 15 seconds for denaturation, and 60°C for 1 minute for annealing/extension. Melt-curve analysis was performed with an initial denaturation at 95°C, followed by a temperature gradient ranging from 60°C to 95°C. To examine the specificity of the primers, each primer set was mixed with genomic DNA from each of the different bacterial species in a 20 µl reaction with 300 nM of primers and qPCR was performed.

Results

SERS spectra on standard substrates with qPCR validation

Acinetobacter baumannii

The average normalized (by vector) SERS spectra of six different *Acinetobacter baumannii* (AB) strains is shown with H_2O as a control (Figure 1). Spectra for the different AB strains were generally similar to the visible eye, with only a few notable differences in terms of peak intensity and peak ratio in the Δv = 730 and 800 cm^{-1} range. In order to better analyze these SERS spectra, principal component analysis (PCA) was conducted as shown (Figure 1B). Utilization of PCA analysis allowed for discrimination and separation of strains AB2, AB3, AB6, and AB7, with AB7 having the greatest discrimination, potentially suggesting a greater difference in morphology as compared to the other AB strains. For strains AB1 and AB4, the difference in spectra was too small to generate discrimination; hence the two strains cluster together following PCA analysis.

SERS data analysis including specificity was validated utilizing qPCR to ensure the correct identification of each specific bacterial species. The Ct value of AB strains AB1, AB2, AB3, AB4, AB6, and AB7 were 21.48, 18.17, 21.97, 14.67, 13.62, and 36.55 respectively, for the *oxa-51* gene specific primer products (Figure 1C). Consistent with the SERS data, all AB strains resulted in early Ct values with strong fluorescent signals except for strain AB7, which generated almost no signal by the end of 40 cycles (Figure 1C) further confirming the genetic differences in AB7 and its uniqueness from the other AB strains. The specificity of the PCR product for all AB strains is shown by a single peak in the melting curves (Figure 2) except for strain AB7 which produces little if any signal, suggesting that strain AB7 may have been misclassified and is not *Acinetobacter baumannii*. The potential cross-reactivity and specificity of the primer sets developed was determined by qPCR amplification, demonstrating amplification of only targeted species (Table 3).

Klebsiella pneumoniae

The average normalized (by vector) spectra of three different *Klebsiella pneumoniae* (KP) strains are shown with H_2O as a control (Figure 3A). With only three strains analyzed, separation of each spectrum was easily achieved via PCA (Figure

3B). The major peaks responsible for such discrimination are found at Δv = 670, 800 and 1030 cm^{-1}. In agreement with the SERS spectra and PCA analysis, qPCR reveals the correct identification of each KP strain with Ct values of 16.11, 12.93, and 16.01 for KP strains KP8, KP9, and KP10 for the *phoE* gene, respectively (Figure 3C). Melt curve analysis reveals a single peak for each strain revealing the specificity of the PCR product (Figure 4).

Pseudomonas aeruginosa

SERS analysis was performed on three *Pseudomonas aeruginosa* (PA) strains. As seen in figure 5A, there is a clear difference in the SERS spectra obtained for strain PA16, as compared to the other two PA strains. Based on our previous experiments, the spectrum of PA16 is a typical spectrum of pyocyanin, a pigment produced by *Pseudomonas aeruginosa* (data not shown). The presence of pyocyanin in the broth is not eliminated by the washing steps; and thus introduces interference into the spectra of the bacteria. Due to this interference, strain PA16 is separated from the other two PA strains in the PCA plot (Figure 5B). Validation of the SERS spectra is observed by qPCR (Figure 5C) with Ct values of 17.12, 18.32, and 15.98 for strains PA14, PA15, and PA16 amplifying up the *rpod* gene, thus verifying the correct identification of the species. Melt curve analysis revealed a single peak demonstrating the specificity of the PCR product (Figure 6).

Staphylococcus aureus

A total of four separate *Staphylococcus aureus* (SA) strains were analyzed by SERS. Apparent differences between the SERS spectra of the *SA* strains resides in the peak ratio at Δv = 730 and 800 cm^{-1} (Figure 7A). Following PCA analysis, strains SA17 and SA22 are seen clustering together, with complete separation of the other two strains, demonstrating the similarities and differences observed in the SERS spectra (Figure 7B). Validation of the SERS results was conducted by qPCR revealing the correct identification of strains SA17, SA18, SA19, and SA22 with Ct values of 14.62, 11.60, 14.83, and 13.99 amplifying the *femA* gene (Figure 7C). Melt curve analysis shows a single peak demonstrating the specificity of a single PCR product (Figure 8).

SERS species level discrimination

The species level discrimination among the SERS spectra of all bacteria isolates were analyzed by PCA (Figure 9). Each species group separated from one another with few strains overlapping. One strain, AB7, showed a high degree of similarity and overlap with bacteria from *Staphylococcus aureus*. This strain, as validated by qPCR could not be amplified with *Acinetobacter baumannii* specific primers, suggesting that the strain may have been previously misclassified. Strains KP8 (*K. pneumoniae*) and SA18 (*S. aureus*) also shared similar SERS spectra based on the proximity of their principal components. Due to the interference in the SERS spectra from the large amount of pyocyanin produced from PA16, this strain was not included in the overall analysis.

Discussion

The lack of a diagnostic platform for the rapid identification and classification of microbial agents continues to have a significant impact on our health care system and wounded warriors. The ability to determine the appropriate therapeutic approach aimed at decreasing morbidity and mortality is greatly needed. Though advances in molecular approaches to detect microorganisms have led to a high-throughput approach to identification, the technical skill sets, mandatory equipment, and prior knowledge of potential microorganisms present, has still hindered these approaches from a true point-of-care field deployable system. In this study, we evaluated the use of a Surface-Enhanced Raman Spectroscopy (SERS)-based platform, followed by principal component analysis algorithms for the rapid identification and classification of bacteria of military significance.

The detection and identification of pathogenic bacteria using a hand-held SERS biosensor system was successful with a level of sensitivity and reproducibility which allowed discrimination down to the bacterial species. The measurement variability for each bacterial strain was evident by the distribution of principal components. The shifts observed in the SERS spectra in terms of the baseline intensity, relative peak intensity, and overall SERS signal amplitude can be attributed to bacterial concentration, orientation, and the contact area of cellular components with the SERS substrates.

The detection time for the SERS biosensor is $\leq$ 30 seconds, which is considerably faster than the gold standards of plating techniques and ribosomal DNA gene sequencing (Esparcia et al., 2011). This rapid species level discrimination of bacteria can be advantageous in circumstances of triage, where addressing infections with highly pathogenic strains of bacteria must be prioritized (Craig et al., 2010). Time of detection, however, does not take into consideration sample preparation time; therefore, reducing or eliminating the need for sample preparation is a grand challenge to SERS-based biosensors and is an active area of research in our lab.

Increases in sensitivity for bacteria detection may be accomplished by altering the surface characteristics of the SERS substrate. For example, solid phase substrates such as the AgNR arrays utilized in this work are amenable to modification with antibiotics such as vancomycin, allowing for SERS detection of bacteria directly from whole blood samples without the need for separation or pre-concentration techniques (Sivanesan et al., 2014). Additionally, modification of AgNR arrays with vancomycin also enhances SERS signal stability and improves the limits of detection down to 10^2 CFU/mL (Wu, Xu, Tripp, Huang, & Zhao, 2013).

It must be noted that the SERS spectra of bacteria presented in this report were collected from fresh cultures and not from biological samples. Compatibility of substrates with biological media such as blood or serum is currently being developed in order to produce a clinically relevant field-deployable biosensor. The species specific and strain specific chemometric models generated in this study lay the foundation for the development of bacteria-specific SERS libraries. Such libraries will be required for generation of algorithms to be used for rapid identification of bacteria with point-of-care devices.

Military Significance

There is a critical, yet currently unmet, need for a rapid and sensitive means of diagnosing microbial agents that can potentially inflict significant burden on our warfighters, including those infected by multidrug-resistant organisms such as methicillin-resistant *Staphylococcus aureus* (MRSA), *Pseudomonas aeruginosa*, *Acinetobacter baumannii*, *Escherichia coli*, and *Klebsiella pneumonia*. Current diagnostic assays used to dictate disease intervention strategies are limited in

sensitivity, have a poor predictive value, or are time-consuming, leading to extended hospital stays and delays in wound recovery. Development of bioanalytical methods that can rapidly, accurately and cost-effectively detect low levels of microbial agents are urgently needed to accelerate therapeutic intervention strategies and protect our troops. The emergence of nanotechnology holds the promise of developing biosensors that allow for the direct, rapid, and sensitive detection of microbial agents of military importance including viruses, bacteria, or microbial products (i.e., spores, toxins, etc.). Recent research has demonstrated that a nanofabrication technique based on glancing angle vapor deposition produces Ag nanorod arrays that exhibit extremely high electromagnetic field enhancements when they are used as Surface-Enhanced Raman Spectroscopy (SERS) substrates. These novel SERS substrates can be used as diagnostic tools to rapidly detect the Raman spectra of biological agents and their products, thus providing unique structural and quantitative information about the agent's "molecular fingerprints". Once generated, microbial agent molecular fingerprinting databases can serve as the foundation for the development of SERS-based diagnostics for utilization of "in theater" applications.

References

Albrecht, M. G., & Creighton, J. A. (1977). Anomalously intense Raman spectra of pyridine at a silver electrode. *Journal of the American Chemical Society, 99*, 5215-5217.

Allain, L. R., & Vo-Dinh, T. (2002). Surface-enhanced Raman scattering detection of the breast cancer susceptibility gene BRCA1 using a silver-coated microarray platform. *Analytica Chimica Acta, 469*(1), 149-154. doi: Pii S0003-2670(01)01537-9 Doi 10.1016/S0003-2670(01)01537-9

Aronson, N. E., Sanders, J. W., & Moran, K. A. (2006). In Harm's Way: Infections in deployed american military forces. *Emerging Infections, 43*, 1045-1051.

Chaney, S. B., Shanmukh, S., Dluhy, R. A., & Zhao, Y. P. (2005). Aligned silver nanorod arrays produce high sensitivity surface-enhanced Raman spectroscopy substrates. *Applied Physics Letters, 87*(3), 031908. doi: 03190810.1063/1.1988980

Chu, H.Y., Huang, Y.W., & Zhao, Y.P. (2008). Silver nanorod array as a SERS substrate for foodborne pathogenic bacteria detection. *Applied Spectroscopy*, revised.

Craig, J. C., Williams, G. J., Jones, M., Codarini, M., Macaskill, P., Hayen, A., . . . McCaskill, M. (2010). The accuracy of clinical symptoms and signs for the diagnosis of serious bacterial infection in young febrile children: prospective cohort study of 15 781 febrile illnesses. *Bmj, 340*.

Driskell, J. D., Shanmukh, S., Liu, Y., Chaney, S. B., Tang, X. J., Zhao, Y. P., & Dluhy, R. A. (2008). The use of aligned silver nanorod Arrays prepared by oblique angle deposition as surface enhanced Raman scattering substrates. *Journal of Physical Chemistry C, 112*(4), 895-901. doi: Doi 10.1021/Jp075288u

Esparcia, O., Montemayor, M., Ginovart, G., Pomar, V., Soriano, G., Pericas, R., . . . Navarro, F. (2011). Diagnostic accuracy of a 16S ribosomal DNA gene-based molecular technique (RT-PCR, microarray, and sequencing) for bacterial meningitis, early-onset neonatal sepsis, and spontaneous bacterial peritonitis. *Diagnostic microbiology and infectious disease, 69*(2), 153-160.

Failloux, N., Bonnet, I., Baron, M. H., & Perrier, E. (2003). Quantitative analysis of vitamin A degradation by raman spectroscopy. *Applied Spectroscopy, 57*(9), 1117-1122. doi: Doi 10.1366/00037020360695973

Faulds, K., Smith, W. E., & Graham, D. (2005). DNA detection by surface enhanced resonance Raman scattering (SERRS). *Analyst, 130*(8), 1125-1131. doi: Doi 10.1039/B500248f

Fleischmann, M., Hendra, P. J., & McQuillan, A. J. (1974). Raman spectra of pyridine adsorbed at a silver electrode. *Chem. Phys. Lett., 26*, 163-166.

Iliescu, T., Cinta, S., & Kiefer, W. (2000). FT-Raman and SERS spectra of rivanol in silver sol. *Talanta, 53*(1), 121-124. doi: Doi 10.1016/S0039-9140(00)00372-6.

Jarvis, R., Clarke, S., & Goodacre, R. (2006). Rapid analysis of microbiological systems using SERS. *Surface-Enhanced Raman Scattering: Physics and Applications, 103*, 397-408.

Jeanmaire, D. L., & Van Duyne, R. P. (1977). Surface Raman spectroelectrochemistry. Part I. Heterocyclic, aromatic, and aliphatic amines adsorbed on the anodized silver electrode. *J. Electroanal. Chem., 84*, 1-20.

Kahraman, M., Yazici, M. M., Sahin, F., Bayrak, O. F., & Culha, M. (2007). Reproducible surface-enhanced Raman scattering spectra of bacteria on aggregated silver nanoparticles. *Applied Spectroscopy, 61*(5), 479-485. doi: Doi 10.1366/000370207780807731

Lecomte, S., & Baron, M. H. (1997). Surface-enhanced Raman spectroscopy investigation of fluoroquinolones-DNA-DNA gyrase-Mg2+ interactions .II. Interaction of pefloxacin with Mg2+ and DNA. *Biospectroscopy, 3*(1), 31-45. doi: Doi 10.1002/(Sici)1520-6343(1997)3:1<31::Aid-Bspy3>3.0.Co;2-V.

Lecomte, S., Moreau, N. J., Manfait, M., Aubard, J., & Baron, M. H. (1995). Surface-enhanced Raman spectroscopy investigation of fluoroquinolone DNA/DNA gyrase Mg2+ interactions .I. Adsorption of pefloxacin on colloidal silver - Effect of drug concentration, electrolytes, and pH. *Biospectroscopy, 1*(6), 423-436. doi: DOI 10.1002/bspy.350010607.

Liu, Y. J., Chu, H. Y., & Zhao, Y. P. (2010). Silver nanorod array substrates fabricated by oblique angle deposition: morphological, optical, and SERS characterizations. *The Journal of Physical Chemistry C, 114*(18), 8176-8183. doi: 10.1021/jp1001644.

Macaskill, A., Chernonosov, A. A., Koval, V. V., Lukyanets, E. A., Fedorova, O. S., Smith, W. E., . . . Graham, D. (2007). Quantitative surface-enhanced resonance Raman scattering of phthalocyanine-labelled oligonucleotides. *Nucleic Acids Research, 35*(6). doi: ARTN e42. DOI 10.1093/nar/gkm042

Mothershed, E. A., & Whitney, A. M. (2006). Nucleic acid-based methods for the detection of bacterial pathogens: present and future considerations for the clinical laboratory. *Clin Chim Acta, 363*, 206-220.

Nomanpour, B., Ghodousi, A., Babaei, A., Abtahi, H., Tabrizi, M., & Feizabadi, M. (2011). Rapid, cost-effective, sensitive and quantitative detection of

Acinetobacter baumannii from pneumonia patients. *Iran J Microbiol, 3*(4), 162-169.

Pal, A., Isola, N. R., Alarie, J. P., Stokes, D. L., & Vo-Dinh, T. (2006). Synthesis and characterization of SERS gene probe for BRCA-1 (breast cancer). *Faraday Discussions, 132*, 293-301. doi: Doi 10.1039/B506341h.

Paule, S. M., Pasquariello, A. C., Hacek, D. M., Fisher, A. G., Thomson, R. B., Jr., Kaul, K. L., & Peterson, L. R. (2004). Direct detection of Staphylococcus aureus from adult and neonate nasal swab specimens using real-time polymerase chain reaction. *J Mol Diagn, 6*(3), 191-196.

Pavel, I., Szeghalmi, A., Moigno, D., Cinta, S., & Kiefer, W. (2003). Theoretical and pH dependent surface enhanced Raman spectroscopy study on caffeine. *Biopolymers, 72*(1), 25-37.

Pearman, W. F., & Fountain, A. W. (2006). Classification of chemical and biological warfare agent simulants by surface-enhanced Raman spectroscopy and multivariate statistical techniques. *Applied Spectroscopy, 60*(4), 356-365.

Pinzàru, S. C., Pavel, I., Leopold, N., & Kiefer, W. (2004). Identification and characterization of pharmaceuticals using Raman and surface-enhanced Raman scattering. *Journal of Raman Spectroscopy, 35*(5), 338-346.

Rolain, J. M., Mallet, M. N., Fournier, P. E., & Raoult, D. (2004). Real-time PCR for universal antibiotic susceptibility testing. *J Antimicrob Chemother, 54*, 538-541.

Sagmuller, B., Schwarze, B., Brehm, G., Trachta, G., & Schneider, S. (2003). Identification of illicit drugs by a combination of liquid chromatography and surface-enhanced Raman scattering spectroscopy. *Journal of Molecular Structure, 661*, 279-290. doi: Doi 10.1016/S0022-8260(03)00507-6.

Shanmukh, S., Jones, L., Driskell, J., Zhao, Y.P., Dluhy, R., & Tripp, R. A. (2006). Rapid and sensitive detection of respiratory virus molecular signatures using a silver nanorod array SERS substrate. *Nano Letters, 6*(11), 2630-2636. doi: Doi 10.1021/Nl061666f.

Sivanesan, A., Witkowska, E., Adamkiewicz, W., Dziewit, Ł., Kamińska, A., & Waluk, J. (2014). Nanostructured silver–gold bimetallic SERS substrates for selective identification of bacteria in human blood. *Analyst*.

Streltsov, S., Oleinikov, V., Ermishov, M., Mochalov, K., Sukhanova, A., Nechipurenko, Y., . . . Nabiev, I. (2003). Interaction of clinically important human DNA topoisomerase I poison, topotecan, with double-stranded DNA. *Biopolymers, 72*(6), 442-454. doi: Doi 10.1002/Bip.10479.

Sun, F., Wu, D., Qiu, Z., Jin, M., Wang, X., & Li, J. (2010). Development of real-time PCR systems based on SYBR Green for the specific detection and quantification of Klebsiella pneumoniae in infant formula. *Food Control, 21*(4), 487-491. doi: http://dx.doi.org/10.1016/j.foodcont.2009.07.014.

Tam, V. H., Schilling, A. N., LaRocco, M. T., Gentry, L. O., Lolans, K., Quinn, J. P., & Garey, K. W. (2007). Prevalence of AmpC over-expression in bloodstream isolates of Pseudomonas aeruginosa. *Clin Microbiol Infect, 13*(4), 413-418.

Vivoni, A., Chen, S. P., Ejeh, D., & Hosten, C. M. (2001). Normal-mode analysis of the Raman-active modes of the anti-tumor agent 6-mercaptopurine. *Journal of Raman Spectroscopy, 32*(1), 1-8. doi: Doi 10.1002/1097-4555(200101)32:1<1::Aid-Jrs655>3.0.Co;2-J.

Vo-Dinh, T., Allain, L. R., & Stokes, D. L. (2002). Cancer gene detection using surface-enhanced Raman scattering (SERS). *Journal of Raman Spectroscopy, 33*(7), 511-516. doi: Doi 10.1002/Jrs.883.

Wang, Y., Li, Y. S., Zhang, Z. X., & An, D. Q. (2003). Surface-enhanced Raman scattering of some water insoluble drugs in silver hydrosols. *Spectrochimica Acta Part a-Molecular and Biomolecular Spectroscopy, 59*(3), 589-594. doi: Pii S1386-1425(02)00213-5Doi 10.1016/S1386-1425(02)00213-5.

Wang, Y., Li, Y. S., Zhang, Z. X., & An, D. Q. (2004). SERS spectra of vitamin A acid in silver solution. *Spectroscopy and Spectral Analysis, 24*(11), 1376-1378.

Wu, X., Xu, C., Tripp, R. A., Huang, Y.W., & Zhao, Y. (2013). Detection and differentiation of foodborne pathogenic bacteria in mung bean sprouts using field deployable label-free SERS devices. *Analyst, 138*(10), 3005-3012.

Tables

Table 1.

Code	Bacteria Strain Name	Strain Number	Code	Bacteria Strain Name	Strain Number
AB1	*Acinetobacter baumannii*	ATCC 19606	KP10	*Klebsiella pneumoniae*	IA- 525
AB2	*Acinetobacter baumannii*	ATTC BAA-1605	PA14	*Pseudomonas aeruginosa*	Xen-41
AB3	*Acinetobacter baumannii*	ATTC 17961	PA15	*Pseudomonas aeruginosa*	BAMC 07- 4
AB4	*Acinetobacter baumannii*	ATTC 19003	PA16	*Pseudomonas aeruginosa*	PA 01
AB6	*Acinetobacter baumannii*	WRAMC #13	SA17	*Staphylococcus aureus*	IQ 0070
AB7	*Acinetobacter baumannii*	WRAMC #19	SA18	*Staphylococcus aureus*	Xen 40
KP8	*Klebsiella pneumoniae*	BAMC 07-18	SA19	*Staphylococcus aureus*	ATCC 33591
KP9	*Klebsiella pneumoniae*	Xen- 39	SA22	*Staphylococcus aureus*	TCH 1516

Table 1. Bacterial Strain Designations. The bacterial strains are listed above with an appropriate abbreviation (code) that is used to reference the strain name throughout the paper.

Table 2.

Species	Gene	Sequence 5'-3'	Reference
A. baumannii	*oxa-51*	Forward 5'-CTCGTGCTTCGACCGAGTAT Reverse 5'-AACCAACACGCTTCACTTCC	(Nomanpour et al., 2011)
K. pneumoniae	*phoe*	Forward 5'-TGCCCAGACCGATAACTTTA Reverse 5'-CTGTTTCTTCGCTTCACGG	(Sun et al., 2010)
P. aeruginosa	*rpod*	Forward 5'-CAGCAATCTCGTCTGAAAGAGTTG Reverse 5' –TTGATCCCCATGTCGTTGATC	(Tam et al., 2007)
S. aureus	*femA*	Forward 5'-AACTGTTGGCCACTATGAGT Reverse 5'-TAAACTTCTTCCGGCACTTCG	(Paule et al., 2004)

Table 2. Primer Sequences for Bacterial Genes for qPCR. The primer nucleotide sequences are listed in the table in the 5' to 3' direction. The gene that they amplify from each species is listed as well along with the reference from which the information for the primers was obtained.

Table 3.

Strain	AB Primers	SA Primers	PA Primers	KP Primers
AB BAA 1605	16.44	---	---	---
SA Xen-40	---	11.22	---	---
PA BAMC 07-4	---	---	13.15	---
KP Xen-39	---	---	---	12.48

Table 3. Cross-Reactivity of Primers. The cross-reactivity of bacterial primers against the other bacterial species is shown in the table above. The (---) denotes no Ct value was detected after 30 cycles. The 'strain' column lists the bacterial strain that was used as the template. The primers used in that reaction are listed under each 'primers' column. The numbers represent the Ct value.

Figures

Figure 1.

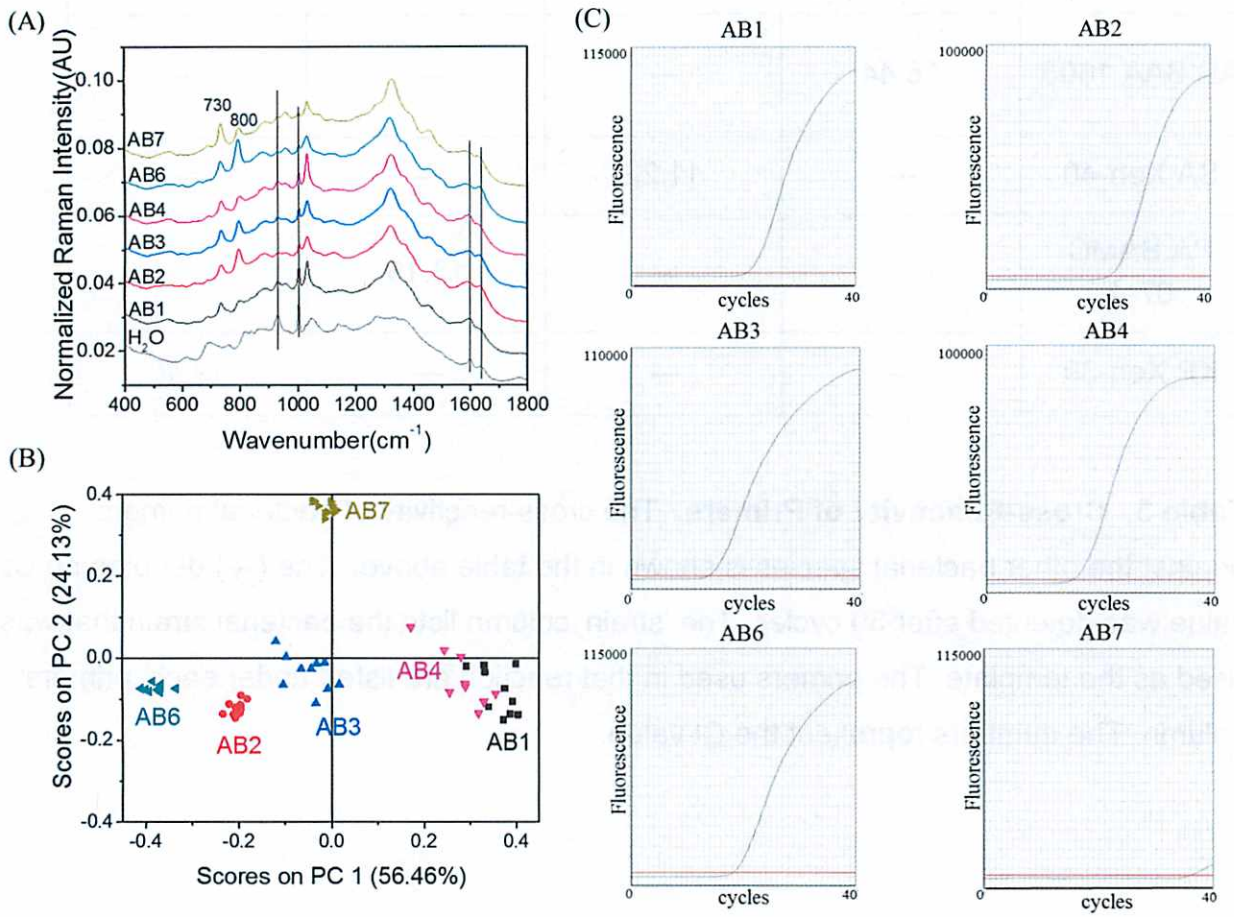

Figure 1. SERS Spectra of *Acinetobacter baumannii* with qPCR Validation.
(A) Average vector normalized SERS spectra of six different *Acinetobacter baumannii* strains with H_2O as control. Y-axis represents the signal intensity, X-axis shows the wavelength. (B) PCA of six different *Acinetobacter baumannii* strains on standard substrates. (C) qPCR verifies the correct identification of the *Acinetobacter baumannii* strains. Y-axis is fluorescence and X-axis is cycle number. The red band represents the noiseband threshold. The cycle number at which the fluorescence crosses the noiseband threshold is the Ct value.

Figure 2.

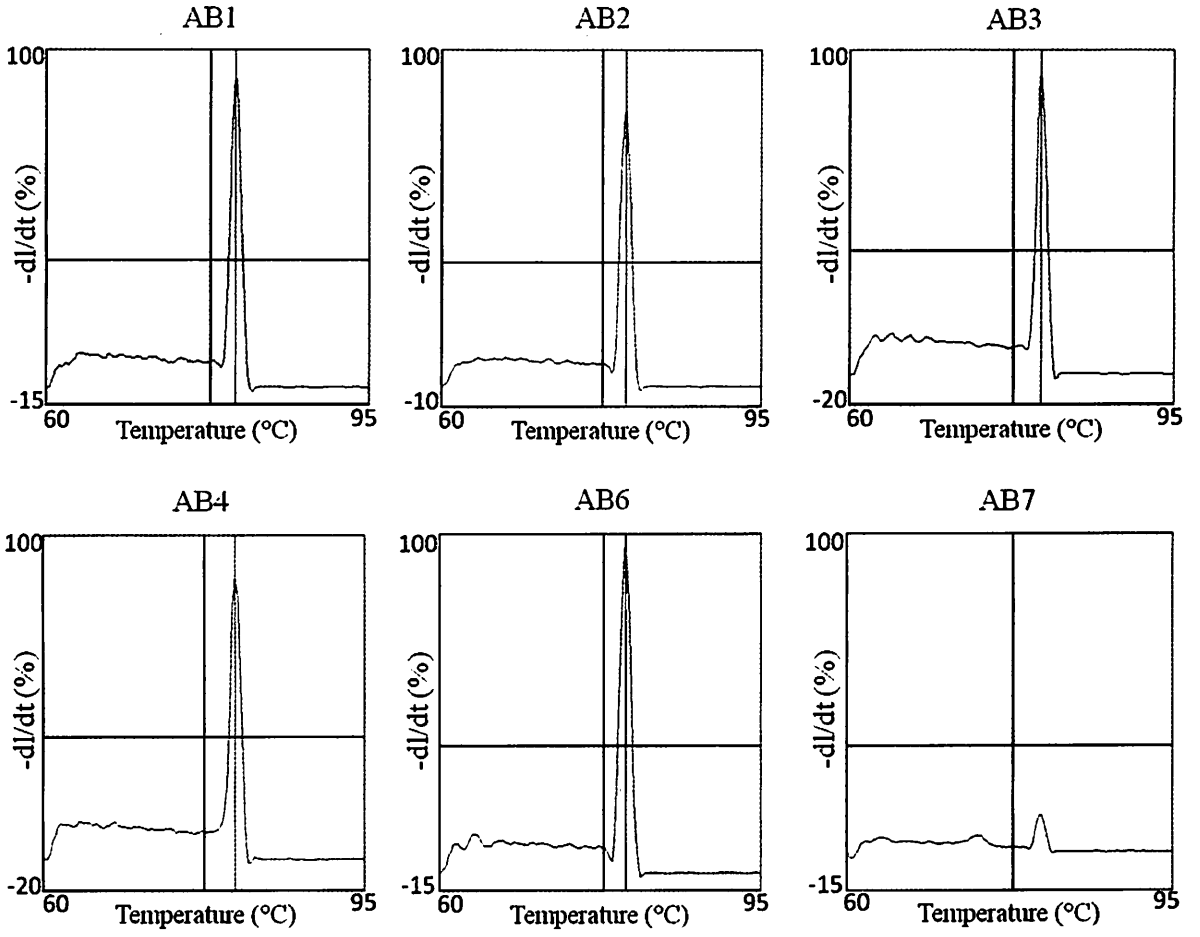

Figure 2. Melting Curves of *A. baumannii* Gene Products. Melt curve analysis from qPCR of the six *Acinetobacter baumannii* strains reveals the presence of a single peak. The y-axis represents the negative first derivative of the melting curves as a function of temperature and is expressed as %, with 100% representing the highest peak of the assay; while the x-axis reveals the temperature. The red band is the threshold which is set at the default setting of 33%. The temperature at which the melting peak is highest is the melting temperature at which 50% of the PCR product has dissociated.

Figure 3.

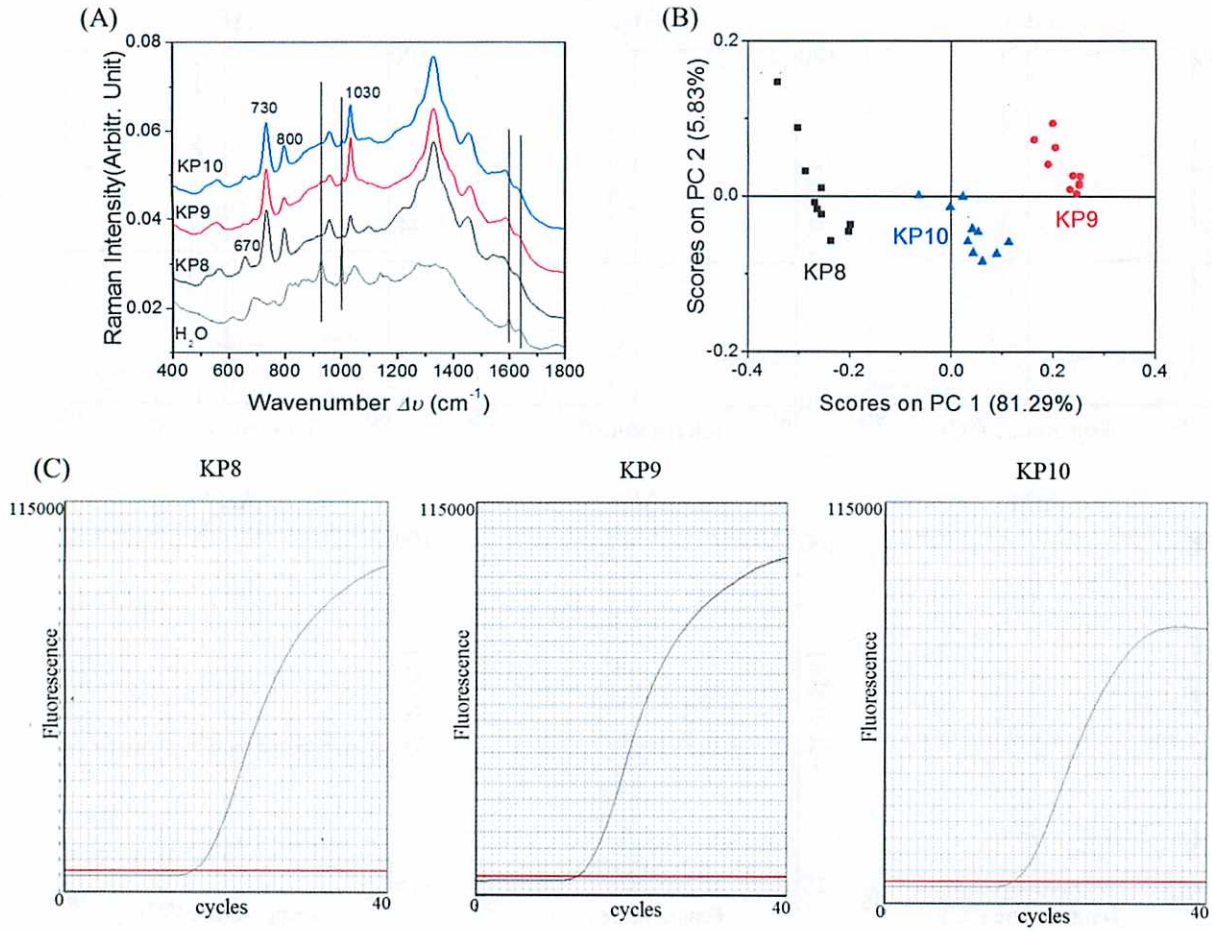

Figure 3. SERS Spectra of *Klebsiella pneumoniae* with qPCR Validation.
(A) Average vector normalized SERS spectra of three different strains of *Klebsiella pneumoniae*. The y-axis represents the signal intensity while the x-axis shows the wavelength. (B) PCA of three different *Klebsiella pneumoniae* strains on standard substrates. (C) qPCR verifies the correct identification of the *Klebsiella pneumoniae* strains. The y-axis is fluorescence and x-axis is cycle number. The red band represents the noiseband threshold. The cycle number at which the fluorescence crosses the noiseband threshold is the Ct value.

Figure 4.

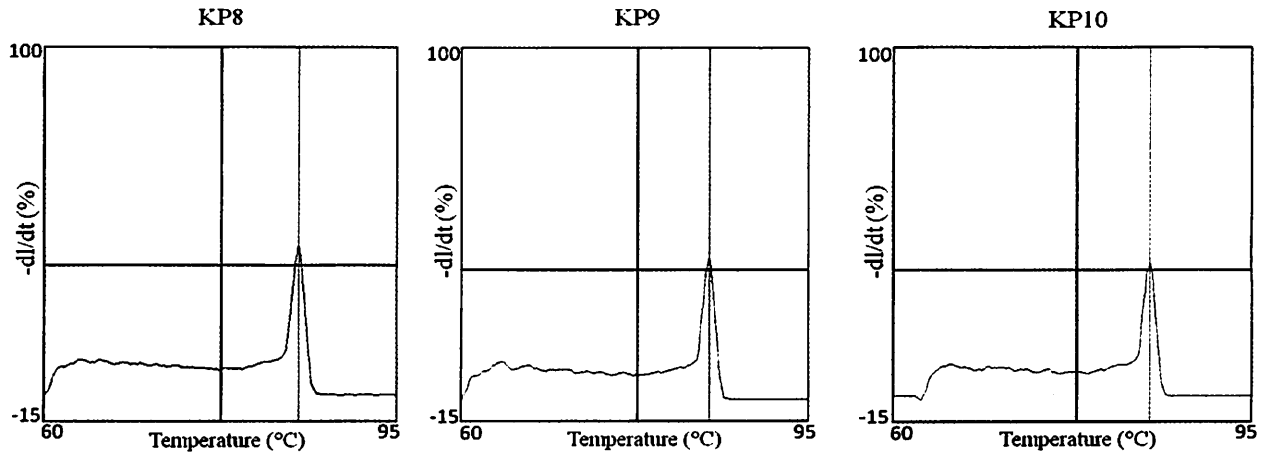

Figure 4. Melting Curves of the *Klebsiella pneumoniae* Strains. Melt curve analysis from qPCR of the three different *Klebsiella pneumoniae* strains demonstrate the specificity of the primers and reveal the presence of a single peak. The y-axis represents the negative first derivative of the melting curves as a function of temperature and is expressed as %, with 100% representing the highest peak of the assay; while the x-axis reveals the temperature. The red band is the threshold which is set at the default setting of 33%. The temperature at which the melting peak is highest is the melting temperature at which 50% of the PCR product has dissociated.

Figure 5.

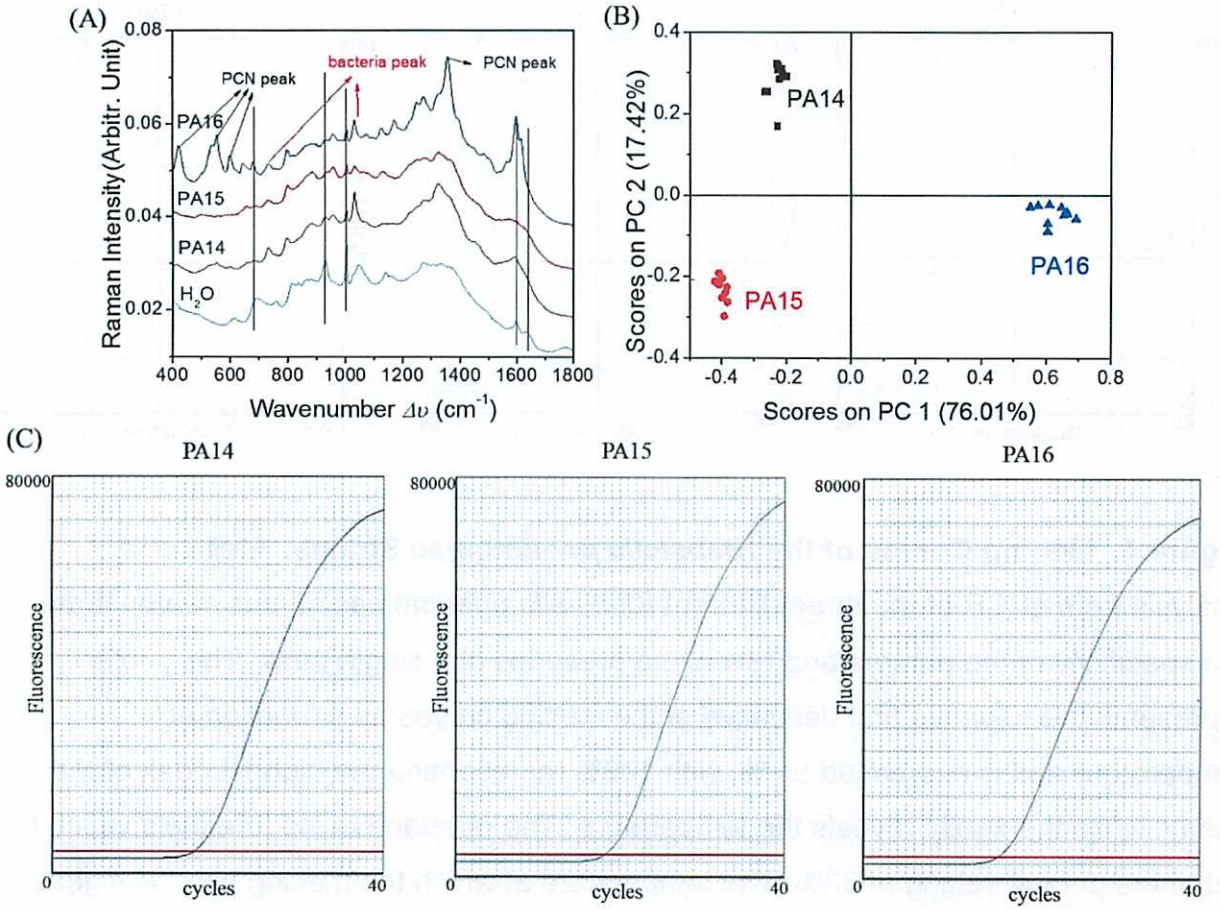

Figure 5. SERS Spectra of *Pseudomonas aeruginosa* with Validation by qPCR. (A) Average vector normalized SERS spectra revealing the three different strains of *Pseudomonas aeruginosa*. The y-axis represents the signal intensity while the x-axis shows the wavelength. (B) PCA of three different *Pseudomonas aeruginosa* strains on standard substrates. (C) qPCR verifies the correct identification of the *Pseudomonas aeruginosa* strains. The y-axis represents fluorescence and x-axis reveals the cycle number. The red band represents the noiseband threshold. The cycle number at which the fluorescence crosses the noiseband threshold equates to the Ct value.

Figure 6.

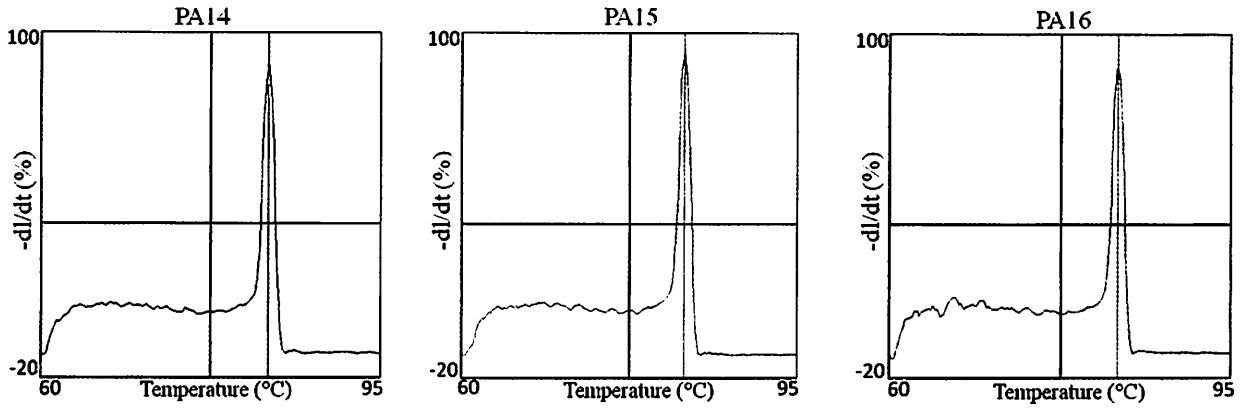

Figure 6. Melting Curves of the *Pseudomonas aeruginosa* Strains. Melt Curve analysis from qPCR reveals the specificity of the primers for the three different *Pseudomonas aeruginosa* strains with the presence of a single melt curve peak. The y-axis represents the negative first derivative of the melting curves as a function of temperature and is expressed as %, with 100% representing the highest peak of the assay; while the x-axis reveals the temperature. The red band is the threshold which is set at the default setting of 33%. The temperature at which the melting peak is highest is the melting temperature at which 50% of the PCR product has dissociated.

Figure 7.

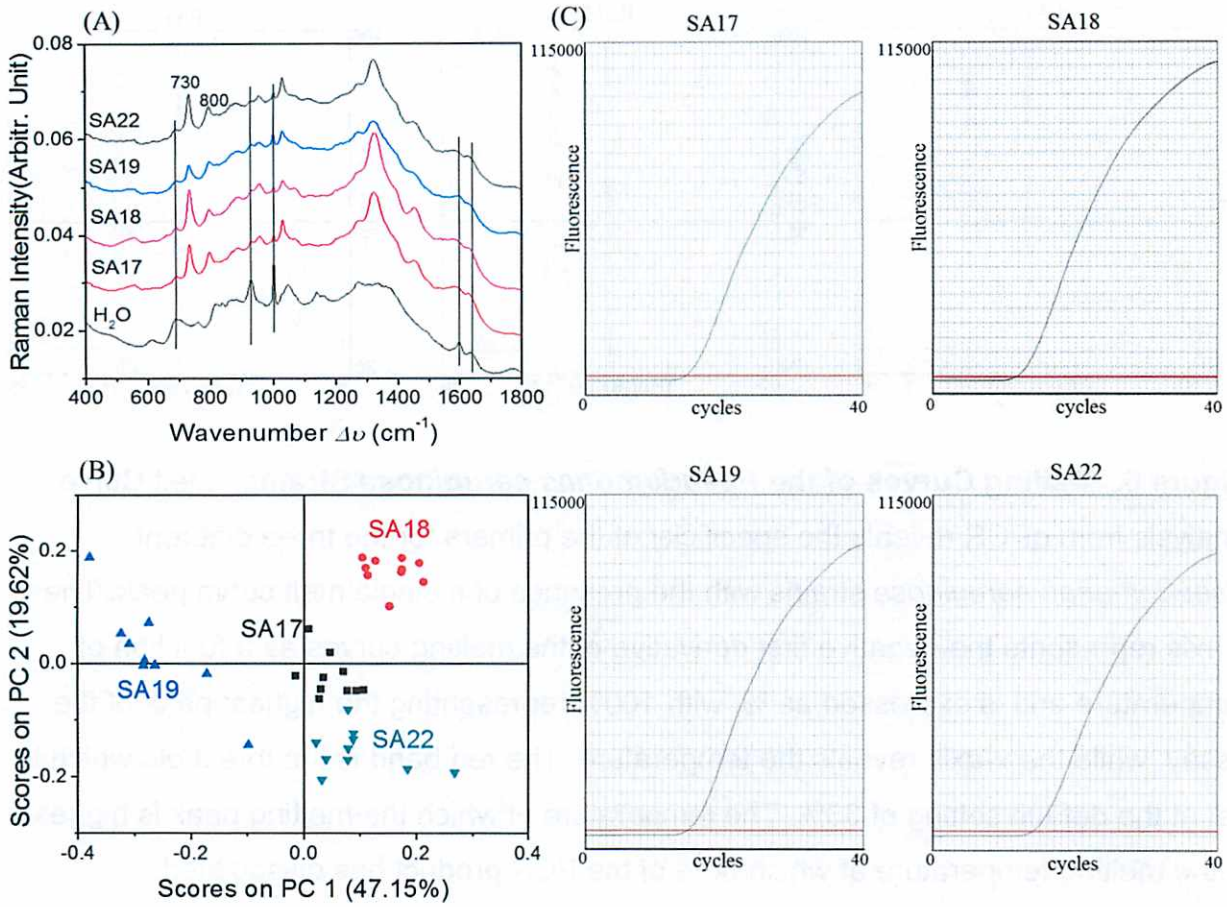

Figure 7. SERS Spectra with qPCR Validation of *Staphylococcus aureus.*

(A) Average vector normalized SERS spectra shows the four different strains of *Staphylococcus aureus*. The y-axis represents the signal intensity while the x-axis shows the wavelength. (B) PCA of four different *Staphylococcus aureus* strains on standard substrates. (C) qPCR verifies the correct identification of the four *Staphylococcus aureus* strains. The y-axis represents fluorescence while the x-axis reveals the cycle number. The red band represents the noiseband threshold. The cycle number at which the fluorescence crosses the noiseband threshold gives the Ct value.

Figure 8.

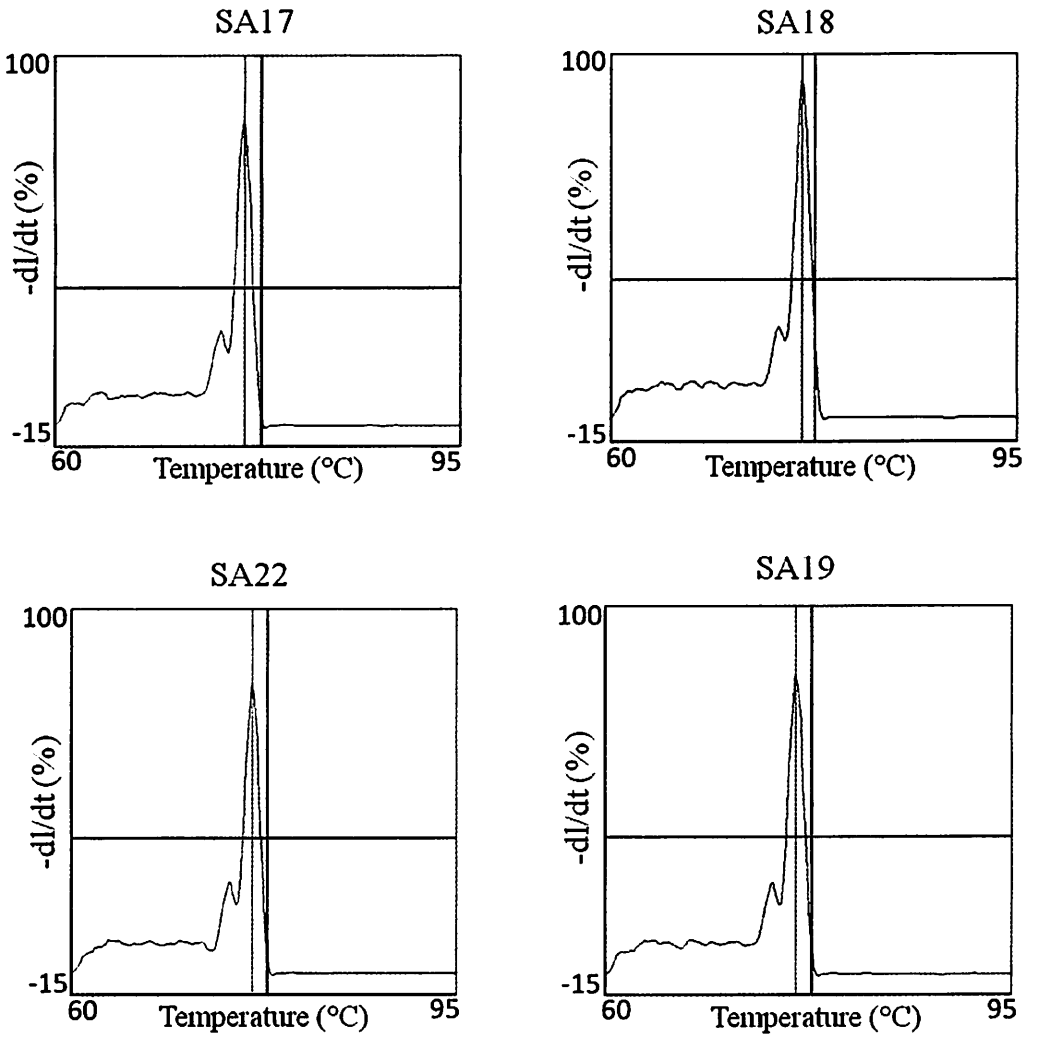

Figure 8. Melt Curve Analysis of the *Staphylococcus aureus* Strains. Melt curve analysis from qPCR of the four different *Staphylococcus aureus* strains shows the specificity of the primers with the presence of a single peak. The y-axis represents the negative first derivative of the melting curves as a function of temperature and is expressed as %, with 100% representing the highest peak of the assay; while the x-axis reveals the temperature. The red band is the threshold which is set at the default setting of 33%. The temperature at which the melting peak is highest is the melting temperature at which 50% of the PCR product has dissociated.

Figure 9.

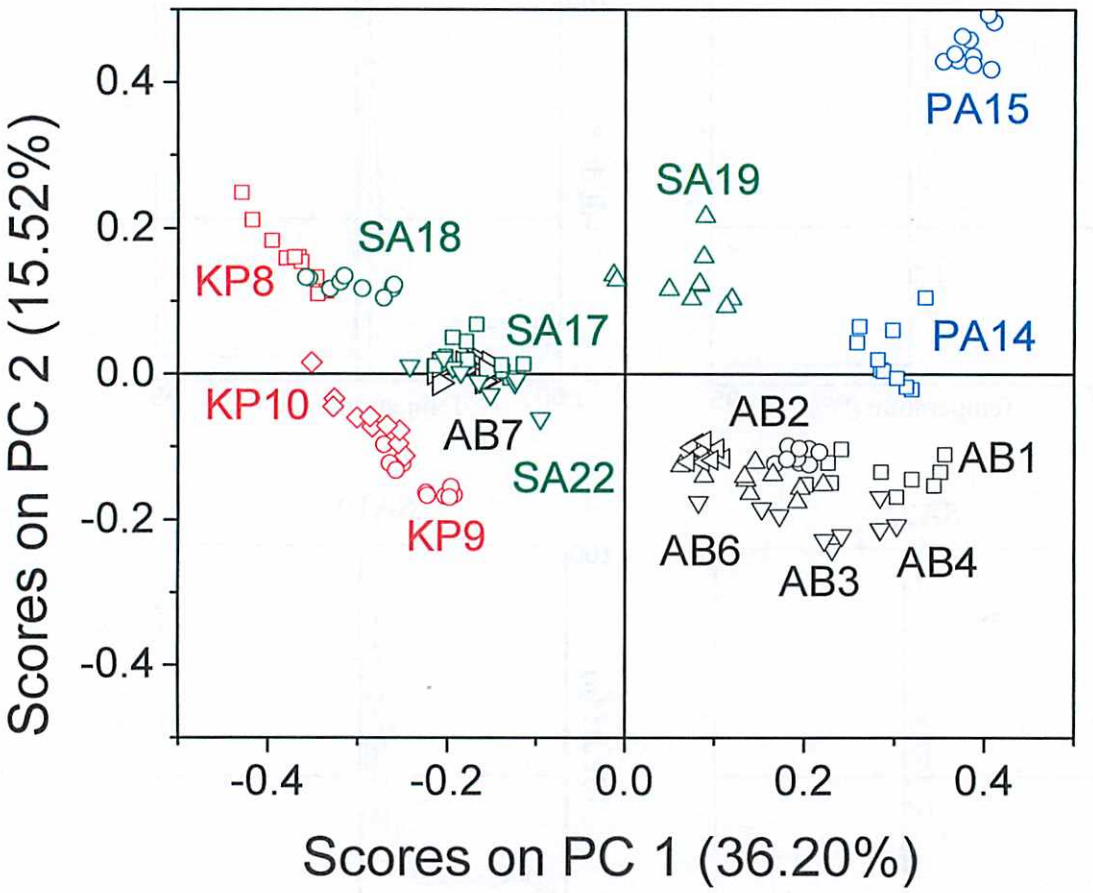

Figure 9. PCA of all 15 Bacterial Strains Together. PCA analysis demonstrates that each group of bacterial species separates out from each other allowing for discrimination between species. PA16 is not shown due to the large pyocyanin peak observed in the spectra.

REPORT DOCUMENTATION PAGE

1. REPORT DATE (DD MM YY)	2. REPORT TYPE	3. DATES COVERED (from – to)
06 11 2014	Joint Technical Report	FY 12 – FY14

4. TITLE
Rapid Identification of Bacterial Pathogens of Military Interest using Surface-Enhanced Raman Spectroscopy

5a. Contract Number:
5b. Grant Number:
5c. Program Element Number:
5d. Project Number:
5e. Task Number:
5f. Work Unit Number: G1011

6. AUTHORS
Rene Alvarez, PhD; Alexander J Burdette, PhD; Xiaomeng Wu, BS; Christian Kotanen, PhD; Yiping Zhao, PhD; Ralph A. Tripp, PhD

7. PERFORMING ORGANIZATION NAME(S) AND ADDRESS(ES)
Naval Medical Research Unit San Antonio
3650 Chambers Pass, BHT-2, Bldg 3610
JBSA, Fort Sam Houston, TX 78234-6315

Department of Physics and Astronomy
University of Georgia, Athens, GA

Department of Infectious Diseases
College of Veterinary Medicine
University of Georgia, Athens, GA

8. PERFORMING ORGANIZATION REPORT NUMBER
Report No. 2014-58

8. SPONSORING/MONITORING AGENCY NAMES(S) AND ADDRESS(ES)
BUMED Core Program / Advanced Medical Development
7700 Arlington Blvd. Suite 5113
Falls Church, VA 22042-5113

10. SPONSOR/MONITOR'S ACRONYM(S)
BUMED

11. SPONSOR/MONITOR'S REPORT NUMBER(s) N/A

12. DISTRIBUTION/AVAILABILITY STATEMENT
Approved for public release; distribution is unlimited.

13. SUPPLEMENTARY NOTES

14. ABSTRACT
The presence of bacterial infections in combat-related injuries in warfighters is becoming increasingly more common and severe. Thus, quick and accurate detection of the invading pathogen is needed so appropriate treatment plans can be generated to improve the prognosis of wounded warriors. The purpose of this study was to evaluate the feasibility of utilizing Surface- Enhanced Raman Spectroscopy (SERS) for the detection and generation of "molecular fingerprints" of military relevant microorganisms often associated with wound infections. A total of sixteen bacterial isolates including: six *Acinetobacter baumannii,* four *Staphylococcus aureus,* three *Klebsiella pneumonia,* and three *Pseudomonas aeruginosa* strains were evaluated for the generation of SERS-based "molecular fingerprints" followed by Principal Component Analysis to determine the uniqueness and commonalities of each spectra. Quantitative polymerase chain reaction (qPCR) with melting curves was used to validate the SERS spectra. Our data demonstrate that SERS could not only generate unique "molecular fingerprints" for these organisms in 15-30 seconds, but could also appropriately group organisms based on commonalities. These data were confirmed by quantitative real-time PCR amplification utilizing species specific primers. Study results demonstrate the valuable potential for a SERS-based platform to rapidly detect microorganisms of military significance. The data demonstrate that SERS can be used to accurately discriminate between bacterial species in a quick and efficient manner. This report sets the foundation for the utilization of a SERS platform for rapid detection of microorganisms of military relevance, which may ultimately lead to the development of a field deployable point-of-care handheld detection system.

15. SUBJECT TERMS
surface-enhanced raman spectroscopy, bacterial infections, rapid identification

16. SECURITY CLASSIFICATION OF:			17. LIMITATION OF ABSTRACT	18. NUMBER OF PAGES	18a. NAME OF RESPONSIBLE PERSON
a. REPORT	b. ABSTRACT	c. THIS PAGE			Commanding Officer
UNCL	UNCL	UNCL	UNCL	31	18b. TELEPHONE NUMBER (INCLUDING AREA CODE) COMM/DSN: 210-539-5334 (DSN: 389)